

Inherent spin density wave instability by vortices in superconductors with strong Pauli effects

K. M. Suzuki, M. Ichioka, and K. Machida

Department of Physics, Okayama University, Okayama 700-8530, Japan

(Dated: November 14, 2018)

A novel spin density wave (SDW) instability mechanism enhanced by vortices under fields is proposed to explain the high field and low temperature (HL) phase in CeCoIn₅. In the vortex state the strong Pauli effect and the nodal gap conspire to enhance the momentum resolved spectral weight exclusively along the nodal direction over the normal value, providing a favorable nesting condition for SDW with $\mathbf{Q} = (2k_F, 2k_F, 0.5)$ only under high field (H). Observed mysteries of the field-induced SDW confined within H_{c2} are understood consistently, such facts that \mathbf{Q} is directed to the nodal direction independent of H , SDW diminishes under tilting field from the ab plane, and the SDW transition line in (H, T) has a positive slope.

PACS numbers: 74.70.Tx, 74.25.Uv, 74.20.-z

The competing-order phenomena are a hallmark of strongly correlated systems. This is particular true for superconductors, such as in heavy Fermion materials, high T_c cuprates or pnictides since competing magnetism is deeply rooted to the pairing mechanism itself where an SDW order generically competes or coexists with superconductivity (SC)[1]. Thus it is not entirely surprising to see that applied field induces an SDW in a superconductor. In fact, in La_{1-x}Sr_xCuO₄[2] and CeRhIn₅ under pressure[3] the field induced SDW is observed only for finite fields and is absent at zero field. A remarkable observation in CeCoIn₅ is that the induced SDW is confined exclusively in the superconducting state below the upper critical field H_{c2} [1] (see HL in Fig.3(c)).

Since Abrikosov[4], there have been many studies on vortices in a type II superconductor based on a concept that the vortex core is a featureless rigid cylindrical object filled with the normal electrons. An emergent new concept based on microscopic Bogoliubov-de Gennes or quasi-classical Eilenberger framework is recently revealing a far richer quasi-particle (QP) structure both in real space and reciprocal space which governs a variety of physical characteristics in a type II superconductor under a field[5]. In particular, in a superconductor characterized by an anisotropic gap, including a nodal gap such as a d-wave symmetry, the QP spatial structure is directly or indirectly measured by various experimental methods, such as scanning tunneling microscope (STM) as direct spatial images[6], small angle neutron scattering (SANS) as Fourier-transformed images[7], or field-angle resolved specific heat[8] or thermal conductivity[9]. With this emergent QP concept we would expect to uncover new phenomena.

Here we investigate detailed behaviors of QPs induced by vortices with the nodal gap structure (i.e. $d_{x^2-y^2}$) and the Pauli paramagnetic effect to uncover the origin of the HL phase in a heavy fermion superconductor CeCoIn₅. This has been discussed theoretically from different view points[10–14]. We find generic features of the QP be-

havior, which enables us to draw vivid physical picture, synthesizing the real space and reciprocal space complementary information. This picture, in particular in reciprocal space, leads naturally us to an SDW instability in a high field, which is confined in the superconducting state. The duality of the QP behaviors in real and reciprocal space is a key concept to uncover the origin of the HL phase. Note in passing that in dHvA effect in the superconducting state the QPs executing the cyclotron motion in real space carry information in the original Fermi surface topology in the normal state, evidencing the dual nature of the QPs created around the vortex core.

The mysterious HL phase exists for both H applied to the basal plane ($H\parallel ab$)[15–19] and the c -axis ($H\parallel c$)[20] of the tetragonal crystal. In particular, for $H\parallel ab$ case the mounting evidence[21, 22] shows that an SDW characterizes the HL phase. The HL phase (see Fig.3(c)) appears via a second order phase transition $H_Q(T)$ from the conventional Abrikosov vortex lattice state. Namely the sublattice magnetization of SDW grows continuously at $H_Q(T)$ and disappears abruptly at H_{c2} via a first order transition. The ordering wave vector $Q = (0.45, 0.45, 0.5)$ in the reciprocal vector units is independent of the field directions $H\parallel(1\bar{1}0)$ [21] and $H\parallel(100)$ [22], and independent of the field strength. The phase boundary $H_Q(T)$ between the HL and the Abrikosov state is almost independent of two field directions. $H_Q(T)$ is an increasing function of T . Those features mainly come from the neutron scattering experiments[21, 22] and basically are consistent with other thermodynamic measurements[15] and NMR experiments[17, 18]. Since the pairing symmetry of this material is firmly established as $d_{x^2-y^2}$ type[8, 9], the origin of this HL phase must be tied to (1) the d -wave nature of this system and (2) the vortex state under a field. As for (1) the controversy of the pairing symmetry either $d_{x^2-y^2}$ or d_{xy} is now resolved[9, 23] and there is little doubt for the $d_{x^2-y^2}$ symmetry in CeCoIn₅[8]. As for (2) it is known by SANS experiments[7] that the Pauli paramagnetic effect is indispensable in understand-

ing the anomalous behaviors of the scattering form factor as functions of field strength and temperature. The purpose of this paper is to examine the generic SDW instability enhanced by the presence of vortices under the strong paramagnetic effect on the basis of the full selfconsistent solutions of microscopic quasi-classical Eilenberger equations.

We calculate the spatial structure of the vortex lattice state by quasiclassical Eilenberger theory in the clean limit valid for $k_F \xi \gg 1$ (k_F is the Fermi wave number and ξ is the superconducting coherence length) [5]. The Pauli paramagnetic effects are included through the Zeeman term $\mu_B B(\mathbf{r})$, where $B(\mathbf{r})$ is the flux density of the internal field and μ_B is a renormalized Bohr magneton. The quasiclassical Green's functions $g(\omega_n + i\mu B, \mathbf{k}, \mathbf{r})$, $f(\omega_n + i\mu B, \mathbf{k}, \mathbf{r})$, and $f^\dagger(\omega_n + i\mu B, \mathbf{k}, \mathbf{r})$ are calculated in the vortex lattice state by the Eilenberger equations

$$\begin{aligned} \{\omega_n + i\mu B + \tilde{\mathbf{v}} \cdot (\nabla + i\mathbf{A})\} f &= \Delta \phi g, \\ \{\omega_n + i\mu B - \tilde{\mathbf{v}} \cdot (\nabla - i\mathbf{A})\} f^\dagger &= \Delta^* \phi^* g, \end{aligned} \quad (1)$$

where $g = (1 - f f^\dagger)^{1/2}$, $\text{Reg} > 0$, $\tilde{\mathbf{v}} = \mathbf{v}/v_{F0}$, and the Maki parameter $\mu = \mu_B B_0 / \pi k_B T_c$. $\mathbf{k} = (k_a, k_b, k_c)$ is the relative momentum of the Cooper pair, and \mathbf{r} is the center-of-mass coordinate of the pair. We set the pairing function $\phi(\mathbf{k}) = \sqrt{2}(k_a^2 - k_b^2)/(k_a^2 + k_b^2)$ in $d_{x^2-y^2}$ -wave pairing. We use the Eilenberger units \mathbf{R}_0 and B_0 [24]. The energy E , pair potential Δ and Matsubara frequency ω_l are in units of $\pi k_B T_c$.

The averaged Fermi velocity on the Fermi surface $v_{F0} = \langle v^2 \rangle_{\mathbf{k}}^{1/2}$ where $\langle \dots \rangle_{\mathbf{k}}$ indicates the Fermi surface average. To model the quasi-two dimensional Fermi surface of CeCoIn₅ we use a Fermi surface with warped cylinder-shape coming from the so-called α -orbit (see four cylinders in Fig.3(a)) [25] and the Fermi velocity is given by $\mathbf{v} = (v_a, v_b, v_c) \propto (\cos \theta_k, \sin \theta_k, \tilde{v}_z \sin k_c)$ at the Fermi surface $\mathbf{k} \propto (k_{F0} \cos \theta_k, k_{F0} \sin \theta_k, k_c)$ with $-\pi \leq \theta_k \leq \pi$ and $-\pi \leq k_c \leq \pi$. We set $\tilde{v}_z = 0.5$, thus the anisotropy ratio $\gamma = \xi_c / \xi_{ab} \sim \langle v_c^2 \rangle_{\mathbf{k}}^{1/2} / \langle v_a^2 \rangle_{\mathbf{k}}^{1/2} \sim 0.5$ as observed in CeCoIn₅.

As for selfconsistent conditions, the pair potential is calculated by

$$\Delta(\mathbf{r}) = g_0 N_0 T \sum_{0 < \omega_n \leq \omega_{\text{cut}}} \left\langle \phi^*(\mathbf{k}) \left(f + f^{\dagger*} \right) \right\rangle_{\mathbf{k}} \quad (2)$$

with $(g_0 N_0)^{-1} = \ln T + 2T \sum_{0 < \omega_n \leq \omega_{\text{cut}}} \omega_l^{-1}$. We use $\omega_{\text{cut}} = 20 k_B T_c$. The vector potential for the internal magnetic field is selfconsistently determined by

$$\nabla \times (\nabla \times \mathbf{A}) = \nabla \times \mathbf{M}_{\text{para}}(\mathbf{r}) - \frac{2T}{\kappa^2} \sum_{0 < \omega_n} \langle \tilde{\mathbf{v}} \text{Im} g \rangle_{\mathbf{k}}, \quad (3)$$

where we consider both the diamagnetic contribution of supercurrent in the last term and the contribution of the

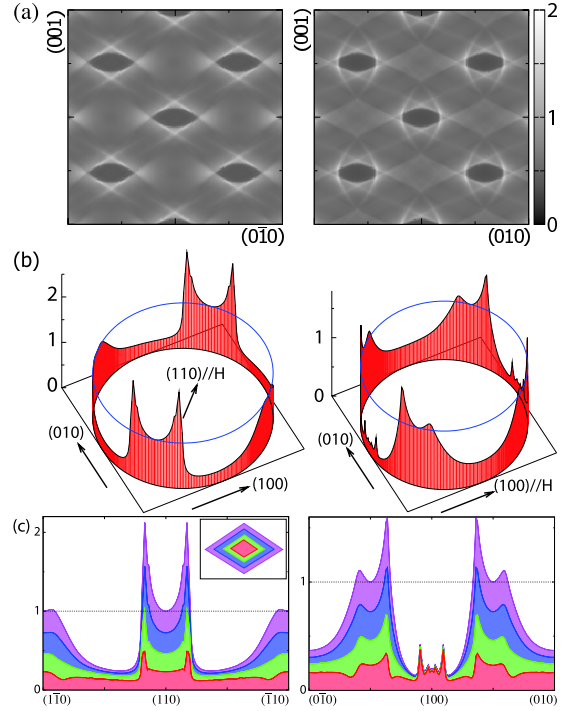


FIG. 1: (Color online) (a) r-DOS $N(\mathbf{r}, E=0)/N_0$ in the real space where vortex cores are placed on the center of each black spot. The view ranges are 16×16 in the Eilenberger unit. (b) k-DOS $N(\mathbf{k}, E=0)/N_0$ on the Fermi surface. Height of the upper rings indicates the normal state value. (c) k-DOS is resolved into the contributed real space areas of one unit cell shown in the inset. Color codes between them coincide. Left column for $H \parallel (110)$ and right for $H \parallel (100)$. $H/H_{c2} = 0.86$, $T/T_c = 0.05$ and $\mu = 2$.

paramagnetic moment $\mathbf{M}_{\text{para}}(\mathbf{r}) = (0, 0, M_{\text{para}}(\mathbf{r}))$ with

$$M_{\text{para}}(\mathbf{r}) = M_0 \left(\frac{B(\mathbf{r})}{H} - \frac{2T}{\mu H} \sum_{0 < \omega_n} \langle \text{Im} g \rangle_{\mathbf{k}} \right). \quad (4)$$

The normal state paramagnetic moment $M_0 = (\mu/\kappa)^2 H$, $\kappa = B_0 / \pi k_B T_c \sqrt{8\pi N_0}$ and N_0 is the density of states (DOS) at the Fermi energy in the normal state. We set the Ginzburg-Landau parameter $\kappa = 89$. We solve eq. (1) and eqs. (2)-(4) alternately, and obtain selfconsistent solutions as in previous works [5] under a given unit cell of the vortex lattice.

The local density of states in real space r-DOS is given by $N(\mathbf{r}, E) = N_\uparrow(\mathbf{r}, E) + N_\downarrow(\mathbf{r}, E)$, where $N_\sigma(\mathbf{r}, E) = \langle N_\sigma(\mathbf{r}, \mathbf{k}, E) \rangle_{\mathbf{k}} = N_0 \langle \text{Re} \{ g(\omega_n + i\sigma \mu B, \mathbf{k}, \mathbf{r}) |_{i\omega_n \rightarrow E+i\eta} \} \rangle_{\mathbf{k}}$ with $\sigma = 1 (-1)$ for up (down) spin component. We typically use $\eta = 0.01$. The total DOS is obtained by the spatial average of the local DOS as $N(E) = N_\uparrow(E) + N_\downarrow(E) = \langle N(\mathbf{r}, E) \rangle_{\mathbf{r}}$. The spectral weight (SW) distribution k-DOS in reciprocal space is given by $N(\mathbf{k}, E) = N_\uparrow(\mathbf{k}, E) + N_\downarrow(\mathbf{k}, E)$ as $N_\sigma(\mathbf{k}, E) = \langle N_\sigma(\mathbf{r}, \mathbf{k}, E) \rangle_{\mathbf{r}}$. Those r-DOS and k-DOS are complimentary, giving rise to valuable information for the QP structures in the vortex state

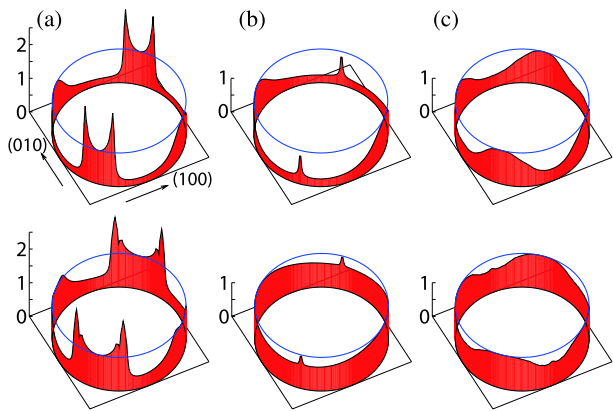


FIG. 2: (Color online) k-DOS $N(\mathbf{k}, E = 0)/N_0$ for low field (upper panel) and high field (lower panel) at $k_z = 0$. (a) For $H \parallel (110)$ with Pauli effect $\mu = 2.0$ where $H/H_{c2} = 0.74$ (upper) and 0.99 (lower). (b) For the absence of Pauli effect $\mu = 0$ where $H/H_{c2} = 0.36$ (upper) and 0.86 (lower). (c) For $H \parallel (001)$ with $\mu = 2.0$ where $H/H_{c2} = 0.77$ (upper) and 0.98 (lower). Height of the upper rings indicates the normal state value. $T/T_c = 0.05$.

as we will see below.

We show the r-DOS at $E = 0$ in Fig. 1(a) and the corresponding k-DOS in Figs. 1(b) and (c) for $H \parallel (110)$ (left column) and $H \parallel (100)$ (right column) for the large paramagnetic effect $\mu = 2$. In Fig. 1(a) we see several characteristic and eminent QP trajectories, notably the bands of the zero energy DOS connecting the nearest neighbor vortex cores. Those real space trajectories correspond to the real space motions of the QP induced by H . It is seen that the zero energy r-DOS is depleted at the vortex core, and piles up in the surrounding area because of the Pauli effect. Due to the Zeeman shift the peak of the zero energy DOS at the vortex core moves up and down in the energy, resulting in the depletion of the zero energy DOS at the core, i.e. the empty core [24]. The zero-energy state moves outside from the core where its maxima occur. Figure 1(b) shows the corresponding k-DOS where on the Fermi circle at $k_z = 0$ the SW for each k-direction is displayed. The SW enhancement along the nodal directions and strong suppression along the antinodal directions are clearly seen for both field orientations. This comes from the real space area surrounding the core, which is seen from Fig. 1(c) where the contribution to the SW enhancement is resolved in the local areas (see inset) with the same areal size. The core area (the central region of the inset) gives a minor contribution because of the empty core.

The field evolutions of the k-DOS are shown in Fig. 2(a) for $H \parallel (110)$ with the strong Pauli effect. As H increases towards H_{c2} , the k-DOS grows with uneven distribution around the Fermi surface, namely the SW is dominated along the nodal direction, keeping suppressed along the antinodal direction. Upon increasing H , the total DOS

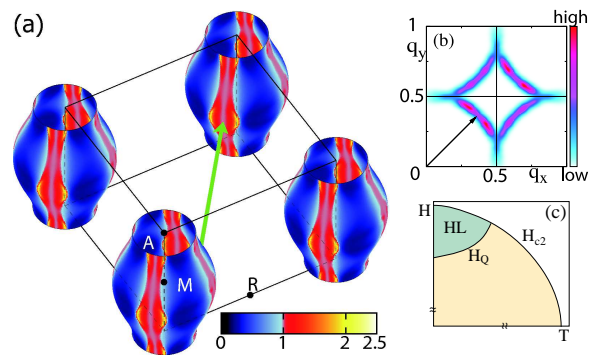


FIG. 3: (Color online) (a) Spectral weight distribution drawn on the Fermi surfaces situated on the four corners of the Brillouin zone. $H/H_{c2} = 0.86$, $T/T_c = 0.05$, $H \parallel (110)$ and $\mu = 2$. Arrow corresponds to $q = 0.05$ when $k_F = 0.26$. (b) Corresponding joint DOS $N_J(\mathbf{q})$. Arrow denotes the best nesting vector \mathbf{Q} in $0 < q_x, q_y < 1.0$ and $q_z = 0.5$, indicating the four maxima $\mathbf{Q} = (0.5 \pm q, 0.5 \pm q, 0.5)$ centered around $(0.5, 0.5, 0.5)$. (c) Schematic phase diagram of the HL phase.

in the vortex state increases towards the normal value at H_{c2} . Because of the Pauli effect, even near H_{c2} the order parameter amplitude is still non-vanishing. Thus beyond a certain H the enhanced SW can exceed the normal value.

It is contrasted with the case for the absence of the Pauli effect ($\mu = 0$) shown in Fig. 2(b) where the order parameter decreases continuously via a second order transition. There, the SW never exceeds the normal value and the SW enhancement never occurs even approaching H_{c2} . Thus the Pauli paramagnetic effect triggers the SDW instability by improving nesting condition. The SW enhancement occurs because under the in-plane field the QP diamagnetic motions are parallel to the k_z -axis, thus they are sensing the nodal lines running along it, giving rise to the singularities in the k-DOS as seen in Fig. 2(a). This one-dimensional QP motion along the nodal line never appears when $H \parallel (001)$ as seen below.

In Fig. 2(c) we display the k-DOS for $H \parallel (001)$. The SW distribution is featureless due to the fact that the QP trajectories in this field orientation traverses the perpendicular nodal line, yielding weakened singularities in the k-DOS. There is no SW enhancement above the normal value for any values of H , implying that the SDW instability is absent in this orientation. Thus by tilting away from $H \parallel (110)$ towards (001) the spectral enhancement ceases to exist. According to our calculation, the critical tilting angle $\theta_{cr} \sim 30^\circ$ from the ab plane. Up to this angle the peak intensity of the k-DOS is maintained. According to Correa, *et al.*[26] the HL phase disappears above $\theta \sim 30^\circ$.

In Fig. 3(a) we display the 3D views of the SW distributions on the α -Fermi surfaces in CeCoIn_5 . This Fermi surface is situated in the four corner of the Brillouin zone. It is clear that the best nesting is expected

for $\mathbf{Q} = (q, q, 0.5)$ in reciprocal vector units, where q is evaluated geometrically as $q = 1 - 2k_F$ as indicated by arrows. The k_z component of \mathbf{Q} comes from the warping of the α -Fermi surface along the k_z direction. In fact, the joint density of states (JDOS) defined by $N_J(\mathbf{q}) = \langle N(\mathbf{k}, E = 0)N(\mathbf{q} - \mathbf{k}, E = 0) \rangle_{\mathbf{k}}$, is one of the indicators to check the degree of the nesting condition and whose maximum may signify the SDW instability. The JDOS is presented in Fig. 3(b). The optimal nesting vector appears at $Q = (0.5 \pm q, 0.5 \pm q, 0.5)$ with $q = 0.05$ when we approximate the Fermi wave number as $k_F = 0.26$ of the α -orbit at the $k_z = 0$ plane according to the combined efforts by the dHvA experiment and band calculation[25]. It is not apparent whether the SDW is described by the double Q or the single Q . Theoretically those are equally possible. Experimentally it is desirable to determine it. In particular, for $H \parallel (100)$ those pairs of the nesting vectors are equivalent by symmetry, leading to either double Q structure or single Q structure with two domains. Yet, the existing experiment[22] only observes one of the pair $\mathbf{Q} = (0.5 - q, 0.5 - q, 0.5)$ and $\mathbf{Q} = (0.5 + q, 0.5 + q, 0.5)$.

An SDW instability with the nesting vector \mathbf{Q} could occur beyond a certain high field $H_Q(T)$ and below H_{c2} (see Fig. 3(c) for schematic phase diagram). As H increases towards H_{c2} , the SW enhancement by vortices becomes larger only along the nodal direction and provides the best SDW nesting condition. It occurs through the repulsive interaction U between those induced QPs. The Stoner instability condition; $U\chi(\mathbf{Q}) > 1$ with $\chi(\mathbf{Q})$ static susceptibility of \mathbf{Q} component is fulfilled. Note that $\chi(\mathbf{Q} = 0) = \mu_B^2 N_0$. Since the observed wave length of the SDW modulation is an order of $\sim 5\text{nm}$ and much shorter than $\xi \sim 30\text{nm}$, there is still a possibility for FFLO to occur as advocated by several authors[10–14] because the present SDW polarized along the c -axis [21, 22] does not liberate the penalty due to the Zeeman effect longitudinal to the in-plane fields. The in-plane anisotropy of the transition line $H_Q(T)$ may not be large because the total DOSs for two directions (100) and (110) differ only by at most 0.4%[8]. As increasing T under a fixed H , the peak value of the SW enhancement $N(k, E = 0)$ decreases because of thermal broadening of the singularities of k-DOS. Thus $dH_Q(T)/dT > 0$, coinciding with the observation[15]. Likewise impurities easily kill the singularities, thus doping experiment can be understood where the HL phase area diminishes upon small Cd- and Hg-dopings[27]. As shown above, the tilting field towards the c -axis ceases to induce the SW enhancement above the normal value. This is supported by the recent neutron experiment[28] and by Correa, *et al.*[26]. Therefore the HL phase in the in-plane field is not connected to the HL phase in the c -axis field, implying that the latter cannot be an SDW instability, but may be genuine FFLO. Those are logical conclusions and predictions based on our microscopic calculations.

In summary, by solving the microscopic Eilenberger equations self-consistently with the $d_{x^2-y^2}$ pairing state and strong Pauli paramagnetic effect, we obtain the detailed information on the quasiparticle structures in both real and reciprocal spaces for vortex lattice states. This complementary information allows us to draw a picture that for the in-plane fields the spectral weight is enhanced by vortices for the nodal direction in k-space exceeded above the normal value, and thus signals an SDW instability whose ordering vector directed towards the nodal direction. This kind of the coexistence between SDW and SC with vortices is a novel form confined exclusively inside SC (see Fig.3(c)), which is beyond known coexistence scheme where two orderings compete each other to try to open their own energy gaps on the Fermi surface[29]. The proposed new SDW mechanism may apply other heavy Fermion superconductors, such as Ce_2PdIn_8 [30].

The authors are grateful for insightful discussions with M. Kenzelmann, S. Gerber, J. S. White, J. L. Gavilano, T. Sakakibara, E. M. Forgan, K. Kumagai and R. Ikeda.

-
- [1] C. Pfleiderer, *Rev. Mod. Phys.* **81**, 1551 (2009).
 - [2] B. Lake, *et al.*, *Nature* **415**, 299 (2002). J. Chang, *et al.*, *Phys. Rev. Lett.* **102**, 177006 (2009).
 - [3] G. Knebel, *et al.*, arXiv: 0911.5223.
 - [4] A. A. Abrikosov, *Soviet Phys-JETP* **5**, 1174 (1957).
 - [5] M. Ichioka, *et al.*, *Phys. Rev. B* **59**, 184 and 8902 (1999).
 - [6] H. F. Hess, *et al.*, *Phys. Rev. Lett.* **62**, 214 (1989). N. Nakai, *et al.*, *ibid* **97**, 147001 (2006).
 - [7] A. D. Bianchi, *et al.*, *Science* **319**, 177 (2008).
 - [8] K. An, *et al.*, *Phys. Rev. Lett.* **104**, 037002 (2010).
 - [9] K. Izawa, *et al.*, *Phys. Rev. Lett.* **87**, 057002 (2001).
 - [10] A. Aperis, *et al.*, *Phys. Rev. Lett.* **104**, 216403 (2010).
 - [11] D. F. Agterberg, *et al.*, *Phys. Rev. Lett.* **102**, 207004 (2009).
 - [12] Y. Yanase and M. Sigrist, *J. Phys. Soc. Jpn.* **78**, 114715 (2009).
 - [13] K. Miyake, *J. Phys. Soc. Jpn.* **77**, 123703 (2008).
 - [14] R. Ikeda, *et al.*, *Phys. Rev. B* **82**, 060510(R) (2010).
 - [15] A. D. Bianchi, *et al.*, *Phys. Rev. Lett.* **91**, 187004 (2003).
 - [16] K. Kakuyanagi, *et al.*, *Phys. Rev. Lett.* **94**, 047602 (2005).
 - [17] G. Koutroulakis, *et al.*, *Phys. Rev. Lett.* **101**, 047004 (2008).
 - [18] B. -L. Young, *et al.*, *Phys. Rev. Lett.* **98**, 036402 (2007).
 - [19] T. Watanabe, *et al.*, *Phys. Rev. B* **70**, 020506(R) (2004).
 - [20] K. Kumagai, *et al.*, *Phys. Rev. Lett.* **97**, 227002 (2006).
 - [21] M. Kenzelmann, *et al.*, *Science* **321**, 1652 (2008).
 - [22] M. Kenzelmann, *et al.*, *Phys. Rev. Lett.* **104**, 127001 (2010).
 - [23] H. Aoki *et al.*, *J. Phys. Condens. Matter* **16**, L13 (2004).
 - [24] M. Ichioka and K. Machida, *Phys. Rev. B* **76**, 064502 (2007).
 - [25] H. Shishido, *et al.*, *J. Phys. Soc. Jpn.* **71**, 162 (2002).
 - [26] V. F. Correa, *et al.*, *Phys. Rev. Lett.* **98**, 087001 (2007).
 - [27] Y. Tokiwa, *et al.*, *Phys. Rev. Lett.* **101**, 037001 (2008).
 - [28] E. Blackburn, *et al.*, preprint.
 - [29] K. Machida and M. Kato, *Phys. Rev. Lett.* **58**, 1986

(1987). K. Machida, J. Phys. Soc. Jpn. **50**, 2195 (1981). [30] J. K. Dong, *et al*, arXiv:1008.0679.
K. Machida and T. Matsubara, *ibid* **50**, 3231 (1981).